Environ Monit Assess (2022) 194: 573
https://doi.org/10.1007/s10661-022-10136-2

Hydrochemical characteristics and formation mechanisms of groundwater in west Zoucheng City, Shandong Province, China

Hao Chen · Jiading Wang · Fei Zhang · Yaxing Zhou · Chunying Xia · Wenliang Zhang · Xianzhou Meng · Jia Meng

Received: 9 August 2021 / Accepted: 26 May 2022 / Published online: 8 July 2022

Abstract Groundwater is an important water source for domestic, industrial, and agricultural use in the western part of Zoucheng, China. Understanding its hydrochemical characteristics and formation mechanisms is important for the sustainable development and utilization of groundwater. In this study, 36 water samples were collected during the wet and dry seasons, respectively, and the hydrochemical components such as K^+, Na^+, Ca^{2+}, Mg^{2+}, Cl^-, SO_4^{2-}, HCO_3^-, NO_3^-, F^-, TH, and TDS were analyzed. A graphical method, correlation analysis, and principal component analysis were applied to explore the hydrochemical characteristics and evolution mechanisms of groundwater in the study area. The results show that the orders of the anion and cation concentrations of karst groundwater and pore groundwater are $Ca^{2+} > Na^+ > Mg^{2+} > K^+$ and $HCO_3^- > SO_4^{2-} > Cl^- > NO_3^- > F^-$, respectively. On the whole, the karst groundwater quality is better than the pore groundwater quality, which in turn is better than the surface water quality. In addition, water quality in the dry season is better than water quality in the wet season for all the three water sources. The hydrochemical types of groundwater are complex and changeable. Compared with dry seasons, HCO_3 and SO_4 type water increase during the wet seasons, while the Cl type and Mg type water decrease. Na type is significantly more prevalent in pore groundwater than in karst groundwater. The chemical formations of karst groundwater and pore groundwater in the dry and wet seasons are mainly affected by water–rock interactions and human activities.

Keywords Karst groundwater · Hydrochemical characteristics · Formation mechanism · Principal component analysis · Zoucheng City

H. Chen · J. Wang (✉)
State Key Laboratory of Continental Dynamics, Department of Geology, Northwest University, Xi'an 710069, China
e-mail: wangjd@nwu.edu.cn

H. Chen · F. Zhang · Y. Zhou · C. Xia · W. Zhang · X. Meng · J. Meng
Shandong Provincial Lunan Geology and Exploration Institute, Jining 272100, Shandong, China

H. Chen · F. Zhang · Y. Zhou · C. Xia · W. Zhang · X. Meng · J. Meng
Key Laboratory of Karst Geology, Shandong Provincial Bureau of Geology and Mineral Resources, Jinan, China

Karst groundwater is one of three types of groundwater. In northern China, unconfined or shallow karst groundwater is usually abundant and of good quality. It is a major source of water for urban and rural residents, irrigation, and important industrial and mining enterprises (He et al., 2019; Liang & Zhao, 2018). Therefore, karst groundwater is an important factor for socio-economic development and improving the standard of living in northern China. Understanding the hydrochemical characteristics of karst groundwater helps facilitate the proper development and

utilization of karst groundwater (Yang et al., 2016). The hydrochemical characteristics of karst groundwater are affected by many factors, such as its sedimentary environment, the chemical composition of precipitation water, ion exchange, water–rock interactions, and human activities (Li et al., 2019; Liu et al., 2018; Luo et al., 2018; Sheng et al., 2013; Wang et al., 2015; Yuan et al., 2016).

Because of its special sensitivity, karst groundwater is more vulnerable than any other type of groundwater. Many researchers have used classic hydrochemical methods and statistical theory to investigate karst groundwater hydrochemistry, its influencing factors, and how best to protect karst groundwater resources (Civita, 2008; Escolero et al., 2002; Hassen et al., 2016; Maramathas, 2006; Plagnes & Bakalowicz, 2002; Reddy & Kumar, 2010; Zang et al., 2015). In these studies, factor analysis techniques and graphical methods were often used to explain correlations among variables and to understand the hydrochemical processes of groundwater. For instance, Smith et al. (2020) used the trilinear Durov plot to investigate the effects of land use on groundwater quality in a karstic aquifer. Lü et al. (2020) evaluated the characteristics and influencing factors of hydrochemistry and dissolved organic matter using statistical analyses in the southwest of Hunan Province, China. Sheikhy Narany et al. (2019) integrated classic geochemical methods and multivariate statistical analysis to demonstrate that the hydrofacies correlate directly with the lithofacies (dolomite). In recent years, isotopic methods have increasingly been used to study the origins of groundwater. Deiana et al. (2018) applied $\delta^{18}O$-δ^{2} H and $^{87}Sr/^{86}Sr$ analyses in order to determine that the source of groundwater recharge in the Berceto landslide is local rainwater, and that external contributions from a local stream can be disregarded. Ventura-Houle et al. (2021) utilized δD and $\delta^{18}O$ data to describe how groundwater interacts with geological formations within the El Abra Formation, the most crucial geological-water unit in their study area. The karst groundwater systems in northern China have played a pivotal role in domestic, industrial, and agricultural water use in the west of Zoucheng. As early as 2000, Bu (2000) evaluated the environmental quality of karst groundwater in the study area and reported that the massive exploitation of groundwater and the leakage of severely polluted river water were the main causes for the deterioration of the groundwater quality in the present study area. Since then, karst groundwater has been over-exploited for 20 years in the western Zoucheng, resulting in a series of geological and environmental problems such as water quality deterioration and a sharp drop in water level. However, information on the main factors determining the water hydrochemistry and the influence of water hydrochemistry on the karst water system remains lacking. The formation process of the groundwater chemistry in western Zoucheng is still unclear.

The present study collected surface water, pore groundwater, and karst groundwater samples in the study area during the wet and dry seasons, and comprehensively uses descriptive statistics, Piper diagrams, Gibbs diagrams, correlation analysis, principal component analysis (PCA), and other methods to analyze the chemical characteristics and formation mechanisms of groundwater. The main objectives of this study were to (1) investigate the difference in the hydrochemical characteristics of pore water and karst water and (2) further explore the formation process of groundwater chemistry in the karst area and (3) provide a reference for the sustainable development and utilization of karst groundwater.

Study area

The study area is located in the west of Zoucheng City, Shandong Province, China, with geographical coordinates of 35°06′05″~35°21′48″N and 116°40′14″~117°02′23″E and an area of about 550 km^2. The southern part of the study area is hilly and mountainous with an elevation of 200–300 m. The southwestern section of the study area is adjacent to Nanyang Lake and Dushan Lake. The terrain there is low-lying and the elevation is about 35 m. The plain in front of the mountains slopes gradually from south to north, with an elevation of 40~70 m. The terrain in the area is generally high in the east and south, and low in the west and north.

The study area has a warm temperate and a semi-humid continental monsoon climate. Its main characteristics are four distinct seasons and concentrated precipitation. The multi-year average temperature in the study area (1956~2018) is 14.1 °C; the average annual precipitation is about 710 mm with a maximum of 1263.8 mm (1964) and a minimum of 268.5 mm (1988). The annual precipitation

is concentrated in the summer months from June to September, which account for about 70% of the annual precipitation. The average annual evaporation is about 1900 mm.

The study area has a relatively independent karst groundwater system with obvious boundaries. To the east of the Jiehe-Kanzhuang-Beilonghe line, the magmatic rocks of the Taishan Group are exposed on the east side of the Yishan fault, forming a no-flow boundary. The southern boundary is the outcropping of Archean metamorphic rocks on the north side of the Fushan fault. The northern Ordovician limestone aquifer is buried under the coal-bearing strata north of Shuangcun. It has poor runoff conditions and can be regarded as a flow barrier. In the northwest, coal-bearing strata occur to the west of the Sunshidian fault that can also be regarded as a no-flow boundary. The southwest corner can be considered a boundary with low permeability (Fig. 1). The southern Cambrian Ordovician strata of the karst groundwater system are exposed to the surface while the northern Ordovician strata are hidden under the Quaternary, and the

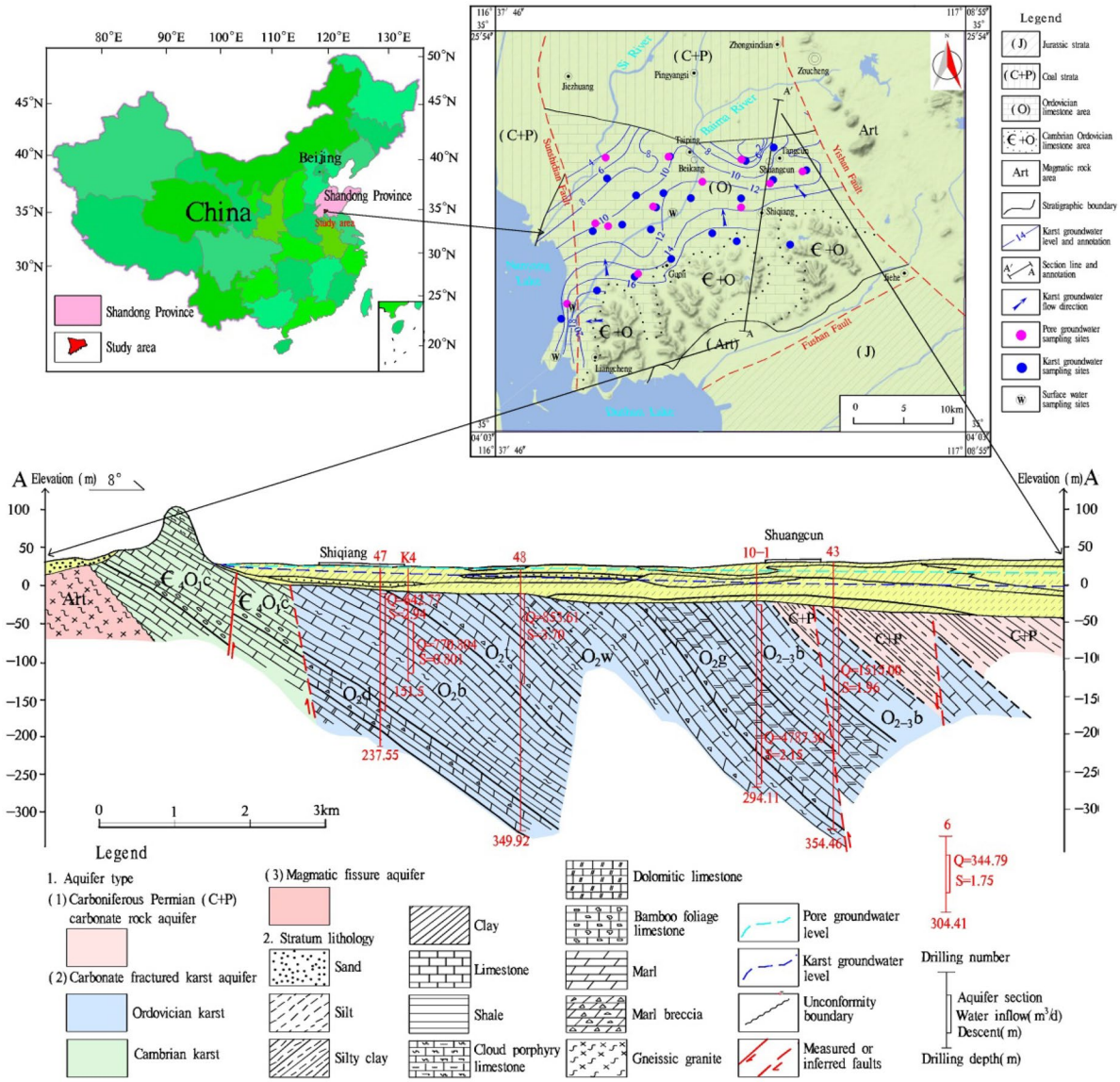

Fig. 1 Map of study area showing sampling locations, geomorphology, hydrogeology, and stratigraphic profile

thickness of the Quaternary gradually increases from south to north, ranging from 0 to 110 m.

The groundwater in the study area is mainly pore groundwater and karst groundwater, of which karst groundwater is the main source for the water supply. The level of pore groundwater is 30 ~ 35 m, and the level of karst groundwater is 0 ~ 10 m. There is no direct connection between the karst and porous aquifer. The burial depth of the karst groundwater gradually increases from south to north, from 10 to 40 m. In the center of exploitation, the dynamic water level can reach more than 50 m below ground. After receiving atmospheric precipitation in the southern hilly area, the karst groundwater generally flows from south to north. Some areas are affected by pumping and groundwater flows towards the pumping center. The pumped water is consumed by the Beikang-Shuangcun-Tangcun area in the northeast of the study area (Fig. 1).

Material and methods

Sample collection and analysis

Thirty-six samples were collected in May (dry season) and another 36 samples were collected in September (wet season) of 2017, including 42 karst groundwater samples, 24 pore groundwater samples, and 6 surface water samples (Fig. 1). The samples were collected in the same wells in the dry and wet seasons. The wells were pumped for a few minutes before taking a water sample to drain the old water from the well pipe. The sampling bottle was rinsed more than 3 times using the pre-sampling product before sampling. The samples were then placed in a thermostat in the sampling vehicle for storage and transportation, and sent to the laboratory on the same day. All samples were analyzed by the Water and Soil Testing Center of the Shandong Provincial Lunan Geology and Exploration Institute. K^+ and Na^+ were determined by flame emission spectrometry, while Ca^{2+}, Mg^{2+}, and TH were determined by EDTA titration. Cl^-, SO_4^{2-}, F^-, and NO_3^- were determined by ion chromatography, and HCO_3^- was determined by titration. TDS values were obtained based on the analysis of data in the lab. The national standard (Ministry of Ecological and Environment, 2009) was used to conduct quality assurance and quality control (QA/QC) of the ion determinations. During the analysis, three replicate water samples were used to assess the precision of the analysis. The analytical precision of the ion charge balance was within 5% for all water samples.

Data analysis method

The Piper diagram and Gibbs diagram were adopted to analyze the water chemistry type and formation effect (He & Li, 2020). GW-Chart Calibration Plots and Surfer software were used to produce the Piper diagram and Gibbs diagram, respectively. SPSS22 helped carry out the statistical analysis, correlation analysis, and principal component analysis. The above results were then combined with geological and hydrogeological data to explore the hydrochemical characteristics and formation mechanism of groundwater in the study area.

Results and discussion

Hydrochemical characteristics

Table 1 shows the chemical composition of karst groundwater, pore groundwater, and surface water in the study area. The order of cation concentration in the karst groundwater during the wet and dry seasons is $Ca^{2+} > Mg^{2+} > Na^+ > K^+$ and $Ca^{2+} > Na^+ > Mg^{2+} > K^+$, respectively, with little difference between Na^+ and Mg^{2+}. The order of anion concentration in the wet and dry seasons is $HCO_3^- > SO_4^{2-} > Cl^- > NO_3^- > F^-$. The order of cation concentrations in the pore groundwater during the wet and dry seasons is $Ca^{2+} > Na^+ > Mg^{2+} > K^+$, which is consistent with the karst groundwater. The order of cation concentrations in the groundwater as a whole in the study area is $Ca^{2+} > Na^+ > Mg^{2+} > K^+$, and that of the anion concentrations is $HCO_3^- > SO_4^{2-} > Cl^- > NO_3^- > F^-$.

During wet and dry seasons, the average concentrations of TDS, Na^+, Mg^{2+}, and Cl^- are the highest in surface water, followed by pore groundwater, and are lowest in karst groundwater. The average concentrations of Ca^{2+}, HCO_3^-, NO_3^-, and TH are the highest in pore groundwater, followed by karst groundwater, and then surface water. Average concentration of K^+ is the highest in surface water, followed by karst groundwater, and then pore groundwater. The

Table 1 Statistics of hydrochemical parameters of groundwater and surface water (mg l^{-}.^{1})

Season	Type	Parameter	TDS	K^+	Na^+	Ca^{2+}	Mg^{2+}	Cl^-	SO_4^{2-}	HCO_3^-	NO_3^-	F^-	TH
Wet	Karst groundwater (n=21)	Mean	643.80	2.53	25.68	138.58	32.04	67.46	162.88	299.08	44.46	0.40	480.87
		Maximum	868.96	15.00	63.53	178.74	57.07	163.63	276.79	412.57	150.82	0.90	618.46
		Minimum	467.62	0.65	6.04	87.24	8.01	17.54	53.04	209.56	3.40	0.04	329.42
	Pore groundwater (n=12)	Mean	890.02	1.73	86.51	162.51	45.64	114.49	209.28	420.01	79.16	1.15	613.07
		Maximum	1796.22	10.00	257.76	255.03	72.37	252.25	706.89	520.26	197.99	3.24	934.93
		Minimum	507.66	0.50	21.18	53.20	10.32	31.72	51.00	181.41	0.12	0.18	308.17
	Surface water (n=3)	Mean	1012.39	9.67	157.85	110.27	45.77	161.26	383.24	235.19	14.99	1.16	463.84
		Maximum	1225.08	11.11	205.91	153.98	55.77	188.17	486.95	259.57	34.76	1.30	614.13
		Minimum	901.14	8.69	117.65	68.93	38.77	117.82	279.84	196.96	0.19	0.97	331.80
Dry	Karst groundwater (n=21)	Mean	532.71	1.72	31.87	122.22	26.96	72.64	156.02	218.94	46.62	0.47	416.21
		Maximum	713.01	8.75	142.50	163.17	82.46	180.83	336.23	376.99	159.02	0.90	711.39
		Minimum	315.52	0.40	4.49	86.16	0.52	17.14	77.59	114.36	10.93	0.10	217.30
	Pore groundwater (n=12)	Mean	721.54	1.11	60.38	125.84	33.78	113.12	144.55	256.80	67.13	0.88	453.32
		Maximum	1265.56	6.25	141.81	215.83	71.99	242.08	455.96	392.59	207.87	3.41	751.07
		Minimum	399.60	0.18	17.69	34.53	1.05	31.45	43.07	127.36	5.63	0.10	213.08
	Surface water (n=3)	Mean	844.87	6.74	167.52	77.80	36.75	170.55	271.70	204.08	3.86	0.83	345.59
		Maximum	895.35	8.00	192.00	116.55	38.26	180.83	335.20	259.99	7.65	0.90	441.92
		Minimum	769.08	5.97	142.50	56.12	35.34	153.31	226.43	171.60	1.04	0.70	285.63

average concentration of SO_4^{2-} is the highest in surface water, followed by pore groundwater, and then karst groundwater in the wet season, and followed by karst groundwater and then pore groundwater during the dry season. The average concentration of F^- is the lowest in karst groundwater, followed by surface water and then pore groundwater during the wet season, and followed by pore groundwater and then surface water in the dry season. In general, karst groundwater quality is better than pore groundwater, and surface water has the worst quality.

The average concentrations of TDS, K^+, Ca^{2+}, Mg^{2+}, SO_4^{2-}, HCO_3^-, and TH in the karst groundwater during the wet season are higher than those found during the dry season, while the other indicators are the opposite. The average concentration of all indicators in the pore groundwater during the wet season is higher than that in the dry season. The average concentrations of all indicators in the surface water are higher in the wet season than in the dry season except for Na^+ and Cl^-, which show the opposite. On the whole, the quality of karst groundwater, pore groundwater, and surface water in the dry season is better than that in the wet season, which may reflect the fact that precipitation carries various ion components into the groundwater during the wet season.

The ion content of karst groundwater shows variations along the karst groundwater flow from the mountainous area in the south to the piedmont plain in the north and northwest (Fig. 2). The concentrations of Na^+, Mg^{2+}, Cl^-, SO_4^{2-}, TDS, and TH in karst groundwater during the wet and dry seasons showed a continuously increasing trend from the mountains to the piedmont plain area, while Ca^{2+}, HCO_3^-, and NO_3^- showed a continuously decreased. Karst groundwater constantly dissolves the ionic components in the rock formations during its migration to the piedmont plains after receiving precipitation in the southern, mountainous area. Therefore, the concentrations of Na^+, Cl^-, SO_4^{2-}, TDS, and TH increase. The steady decrease of Ca^{2+} can be attributed to cation exchange. The reduction of HCO_3^- may

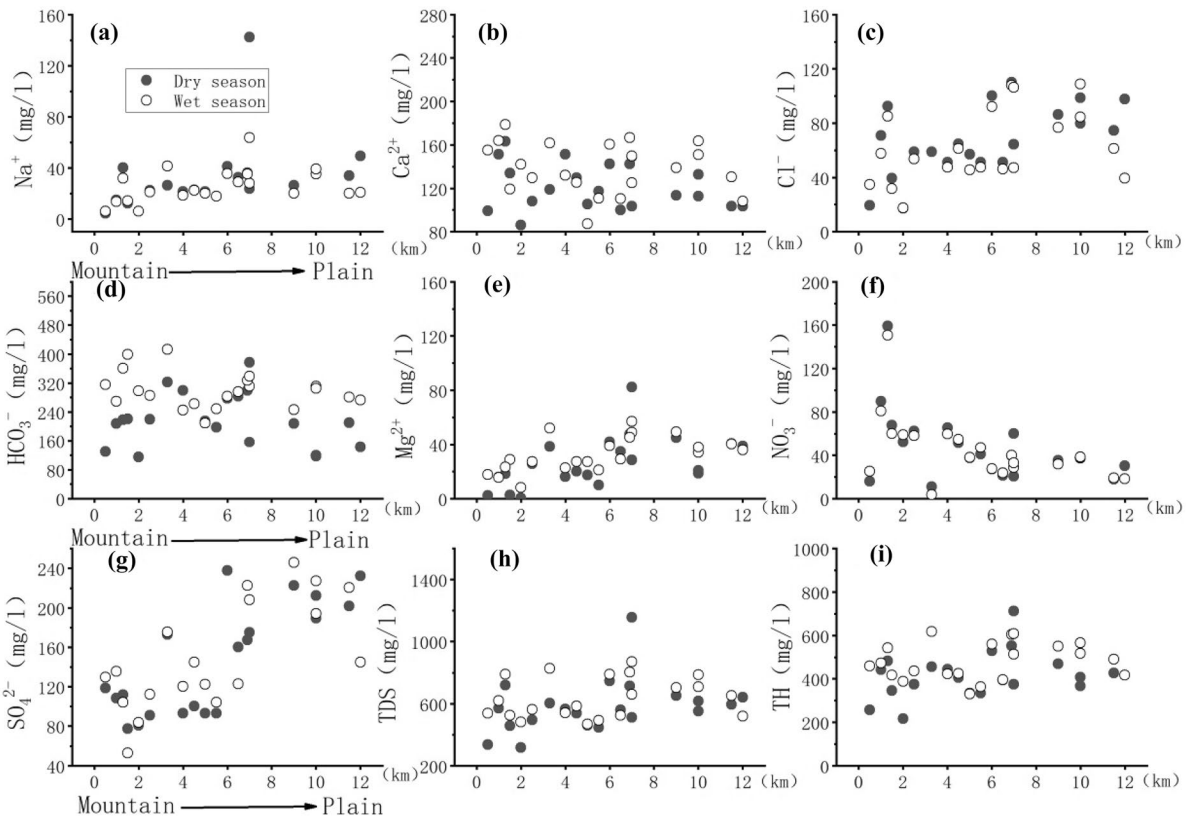

Fig. 2 Spatial distribution of ion content in karst groundwater in the study area (**a–i** represent the spatial distribution of Na^+, Ca^{2+}, Cl^-, HCO_3^-, Mg^{2+}, NO_3^-, SO_4^{2-}, TDS, TH respectively)

be related to the greater depth of the aquifers far away from the mountainous area, because less corrosive CO_2 can lead to less $CaCO_3$ dissolution in limestone or dolomite. The continuous decrease of NO_3^- may be due to the increase in the depth of the karst aquifer. Karst aquifers are not easily affected by human activities on the surface.

In the vertical direction, the variation range of the ion concentration of the upper pore groundwater during the wet and dry seasons is significantly larger than that of the lower karst groundwater, while the ion concentration of the karst groundwater increases slightly with the depth of the well (Fig. 3). The large range of ion changes in the pore groundwater may be

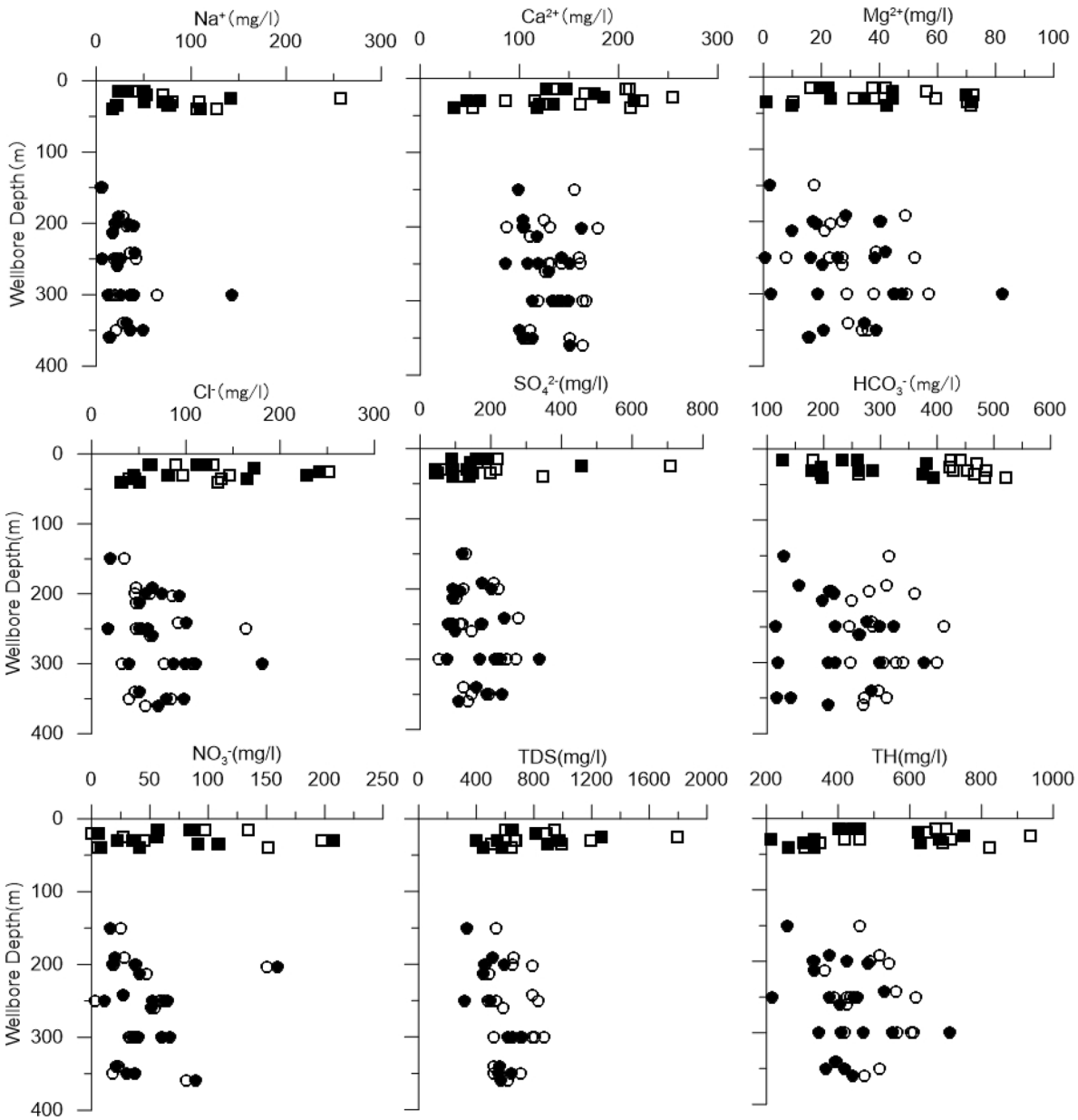

Fig. 3 Vertical distribution of groundwater ion content in the study area

because it is more susceptible to human activities. The increase of ion content in karst groundwater with wellbore depth may be caused by slower runoff due to the greater depth of the well.

Figure 4 shows that there are 7 types of karst groundwater in the dry season, mainly HCO_3-Ca and $HCO_3 \cdot SO_4$-Ca·Mg types. There are 5 types of water in the wet season, mainly $HCO_3 \cdot SO_4$-Ca·Mg and $HCO_3 \cdot SO_4$-Ca types. Compared with the dry season, the HCO_3 and SO_4 types of the karst groundwater during the wet season increased by 14% and 24%, respectively. The significant changes in karst groundwater chemical types between the wet and dry seasons indicate that the groundwater in the southern, mountainous area can quickly drain to the whole study area after receiving a precipitation recharge, so the karst groundwater circulation is faster. Compared with karst groundwater, the chemical types of pore groundwater are more complex, with 10 types in both dry and wet periods. Compared with the dry season, the HCO_3 type of pore groundwater during the wet season increased, and the Cl type and Mg type decreased. The inconsistency of groundwater chemistry types between wet and dry seasons may reflect precipitation recharge. The water chemistry type of surface water is quite different from that of pore

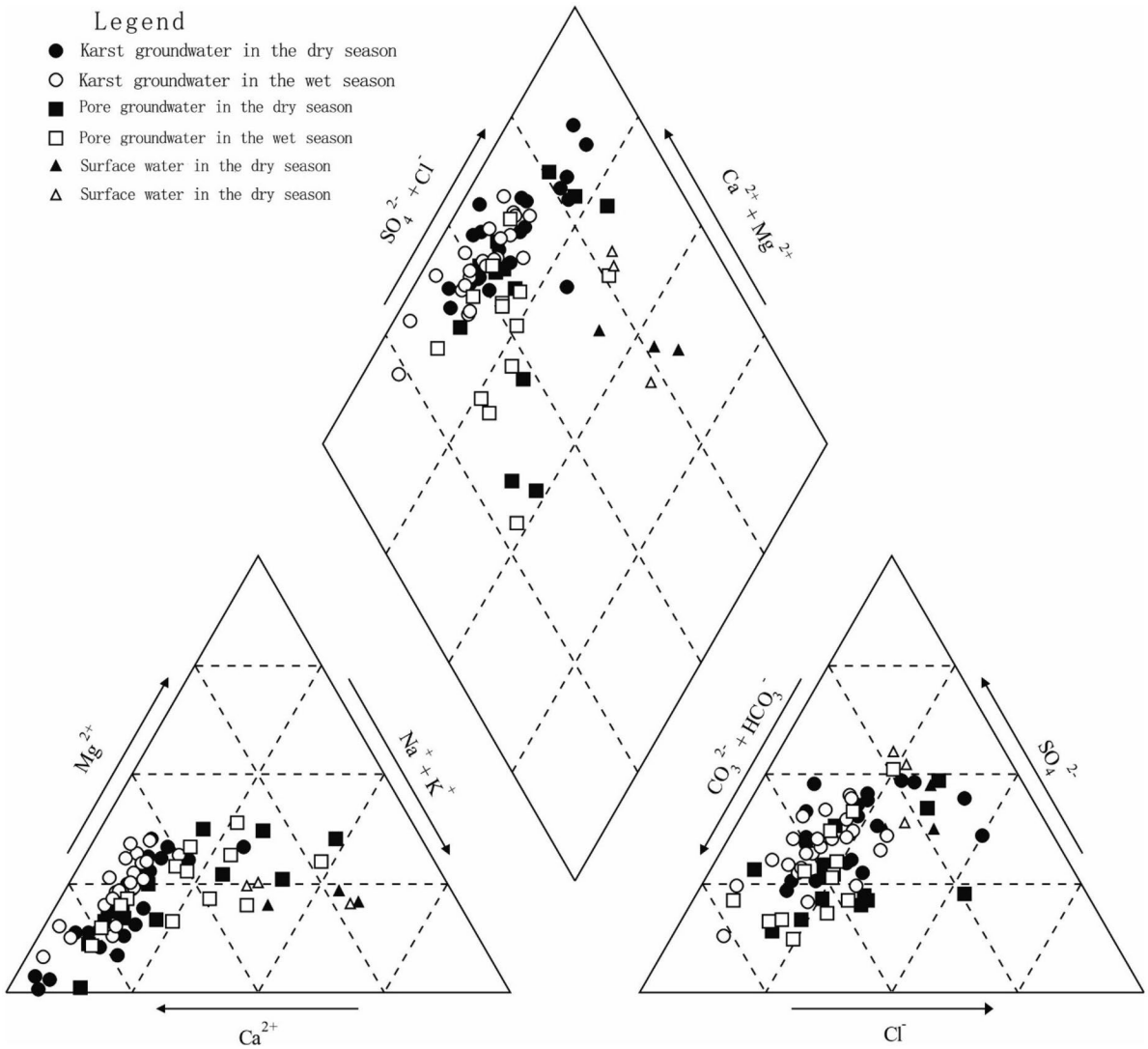

Fig. 4 Piper diagram of groundwater in the study area

groundwater and karst groundwater. There are 2 and 3 types of surface water chemistry in dry season and wet season, respectively, with Cl type and Na type being dominant.

Comparing the hydrochemical types of karst groundwater, pore groundwater, and surface water in the study area, Na type water rarely appears in karst groundwater and only occurs during the dry season of hole J23. However, 33% of pore groundwater and 100% of surface water samples are Na type water. In addition, the hydrochemical types of karst groundwater also show a clear spatial distribution. The southern mountainous area and the intermountain areas directly replenish the karst groundwater, where the groundwater chemistry types are relatively simple, generally HCO_3-Ca and HCO_3·SO_4-Ca types. The northern region of the study area is the drainage area for the karst groundwater. The groundwater chemistry types are complex and changeable there, showing HCO_3·SO_4-Ca·Mg, HCO_3-Ca, SO_4·Cl-Ca, HCO_3·SO_4-Ca, and other types. The complex groundwater chemistry types indicate that the water chemistry characteristics of pore groundwater and karst groundwater are affected by many factors.

Correlation analysis

The origin of solutes can be illustrated by the correlation coefficient within hydrochemical parameters and their correlations are divided into three types: strong ($|r|>0.7$), moderate ($0.5<|r|<0.5$), and weak ($|r|<0.5$) (Lü et al., 2020). Table 2 shows the Pearson correlation coefficients of hydrochemical parameters of the karst groundwater in the study area. TDS is strongly associated with Cl^-, Mg^{2+}, Na^+, and SO_4^{2-} and is moderately associated with Ca^{2+} and HCO_3^- in karst groundwater demonstrating higher TDS due to the presence of these ions. TH shows a strong positive correlation with Mg^{2+}, Cl^-, Ca^{2+}, and HCO_3^- and a moderate positive correlation with SO_4^{2-} and Na^+. Both TDS and TH have weak associations with K^+, F^-, and NO_3^-, indicating that K^+, F^-, and NO_3^- are different from other ions and are mainly affected by human activities in karst groundwater. Cl^- is strongly correlated with Na^+ (correlation coefficient is 0.816), suggesting that weathering of halite is an important process for karst groundwater. HCO_3^- has moderate correlation to Ca^{2+} and Mg^{2+} in karst groundwater, indicating that HCO_3^-, Ca^{2+}, and Mg^{2+} may have the same source. They may originate from the dissolution of calcite and dolomite.

Table 3 shows the Pearson correlation coefficients of the hydrochemical parameters of the pore groundwater. Unlike karst groundwater, TDS is strongly associated with SO_4^{2-}, Cl^-, Ca^{2+}, Na^+, and Mg^{2+} in pore groundwater and is weakly associated with the other parameters. TH shows a strong positive correlation with Ca^{2+}, Cl^-, and SO_4^{2-}, a moderate positive correlation with Mg^{2+}, and a weak correlation with the other parameters in pore groundwater indicating that the dissolution of carbonate rocks is not on the main processes in the formation of pore water. The absence of strong correlations between HCO_3^- and the other parameters indicates that the HCO_3^- type is not predominant in pore groundwater. Cl^- shows

Table 2 Correlation matrices of hydrochemical parameters of karst groundwater

	K^+	Na^+	Ca^{2+}	Mg^{2+}	Cl^-	SO_4^{2-}	HCO_3^-	F^-	NO_3^-	TDS	TH
K^+	1	0.089	0.438**	0.018	0.206	−0.072	0.207	−0.187	0.705**	0.312*	0.275
Na^+		1	0.255	0.751**	0.816**	0.703**	0.303	0.471**	0.016	0.823**	0.663**
Ca^{2+}			1	0.222	0.499**	0.243	0.577**	−0.116	0.434**	0.666**	0.749**
Mg^{2+}				1	0.737**	0.812**	0.524**	0.646**	−0.312*	0.824**	0.812**
Cl^-					1	0.710**	0.326*	0.427**	0.000	0.885**	0.799**
SO_4^{2-}						1	0.145	0.703**	−0.380*	0.766**	0.697**
HCO_3^-							1	0.020	0.046	0.579**	0.701**
F^-								1	−0.461**	0.422**	0.369*
NO_3^-									1	0.101	0.047
TDS										1	0.958**
TH											1

*significant at the 0.05 level (2-tailed); **Significant at the 0.01 level (2-tailed)

Table 3 Correlation matrices of hydrochemical parameters of pore groundwater

	K^+	Na^+	Ca^{2+}	Mg^{2+}	Cl^-	SO_4^{2-}	HCO_3^-	F^-	NO_3^-	TDS	TH
K^+	1	−0.121	0.282	−0.014	0.040	0.030	0.166	−0.284	0.115	0.109	0.207
Na^+		1	0.246	0.682**	0.514*	0.801**	0.438*	0.329	−0.227	0.746**	0.494*
Ca^{2+}			1	0.326	0.749**	0.639**	0.183	−0.551**	0.524**	0.804**	0.904**
Mg^{2+}				1	0.633**	0.609**	0.621**	0.422*	−0.118	0.725**	0.698**
Cl^-					1	0.696**	0.104	−0.196	0.182	0.821**	0.853**
SO_4^{2-}						1	0.197	−0.082	0.004	0.903**	0.759**
HCO_3^-							1	0.334	−0.093	0.424*	0.419*
F^-								1	−0.382	−0.104	−0.226
NO_3^-									1	0.249	0.344
TDS										1	0.936**
TH											1

*significant at the 0.05 level (2-tailed); **Significant at the 0.01 level (2-tailed)

a strong positive correlation with TH, TDS, and Ca^{2+}; a moderate positive correlation with SO_4^{2-}, Mg^{2+}, and Na^+; and a weak correlation with the other parameters.

Formation mechanisms controlling groundwater chemistry

Water–rock interaction

The Gibbs graphic method (Gibbs., 1970) can be used to analyze the role of precipitation, water–rock interaction, and evaporation in the chemical evolution of groundwater (Brindha et al., 2011; Wang et al., 2014; Liu et al., 2015; Bouzourra et al., 2015; Li et al., 2015, 2016; Adimalla, 2019). The karst groundwater, pore groundwater, and surface water in the study area are all located within the dominant area of water–rock interaction in the Gibbs diagram (Fig. 5), indicating that they are all mainly affected by water–rock interaction. Figure 5a shows that Na/(Na + Ca) has the smallest value in karst groundwater, followed by pore groundwater, and surface water has the highest value. Some pore groundwater and surface water are close to the evaporation dominant area and may also be affected by evaporation to some extent.

Karst groundwater mainly occurs in the Ordovician Majiagou Group strata. The lithology of this stratum is dominated by carbonate rocks such as limestone ($CaCO_3$) and dolomite (CaMg (CO_3)). If HCO_3^-, Ca^{2+}, and Mg^{2+} are from the dissolution of carbonate rocks, then HCO_3^- and $Ca^{2+} + Mg^{2+}$ should exist in basically equal amounts, but Fig. 6b shows that the karst groundwater points are all located above the 1:1 line, indicating that the Ca^{2+} and Mg^{2+} have other sources. According to the drilling core data, there is a gypsum layer in the area. The dissolution of the gypsum will also increase the Ca^{2+} in karst groundwater. Figure 6c shows that the karst groundwater sample points are all distributed near the 1:1 line, further confirming that the HCO_3^-, SO_4^{2-}, Ca^{2+}, and Mg^{2+} in the karst groundwater come from the dissolution of limestone, dolomite, and gypsum.

Most of the karst groundwater samples from the wet season are located to the upper right side of those from the dry season (Fig. 6b, c), indicating that the content of HCO_3^-, Ca^{2+}, and Mg^{2+} in the wet season is higher than that during the dry season. This may be related to rainfall carrying CO_2 into the karst groundwater during the wet season, which promotes the dissolution of carbonate rocks.

Cation exchange

The correlation between (Na^+–Cl^-), [($Ca^{2+} + Mg^{2+}$)–($HCO_3^- + SO_4^{2-}$)], and the chlor-alkali index (CAI-1, CAI-2) can be used to explain the cation exchange effect (Li et al., 2019, 2016; Marghade et al., 2012; Rajesh et al., 2015; Salem et al., 2015). When cation exchange is the main factor affecting the formation of groundwater chemistry, the relationship between (Na^+–Cl^-) and [($Ca^{2+} + Mg^{2+}$)–($HCO_3^- + SO_4^{2-}$)] is linear, and the slope is close to −1. The correlation equations of karst groundwater in the wet and dry seasons

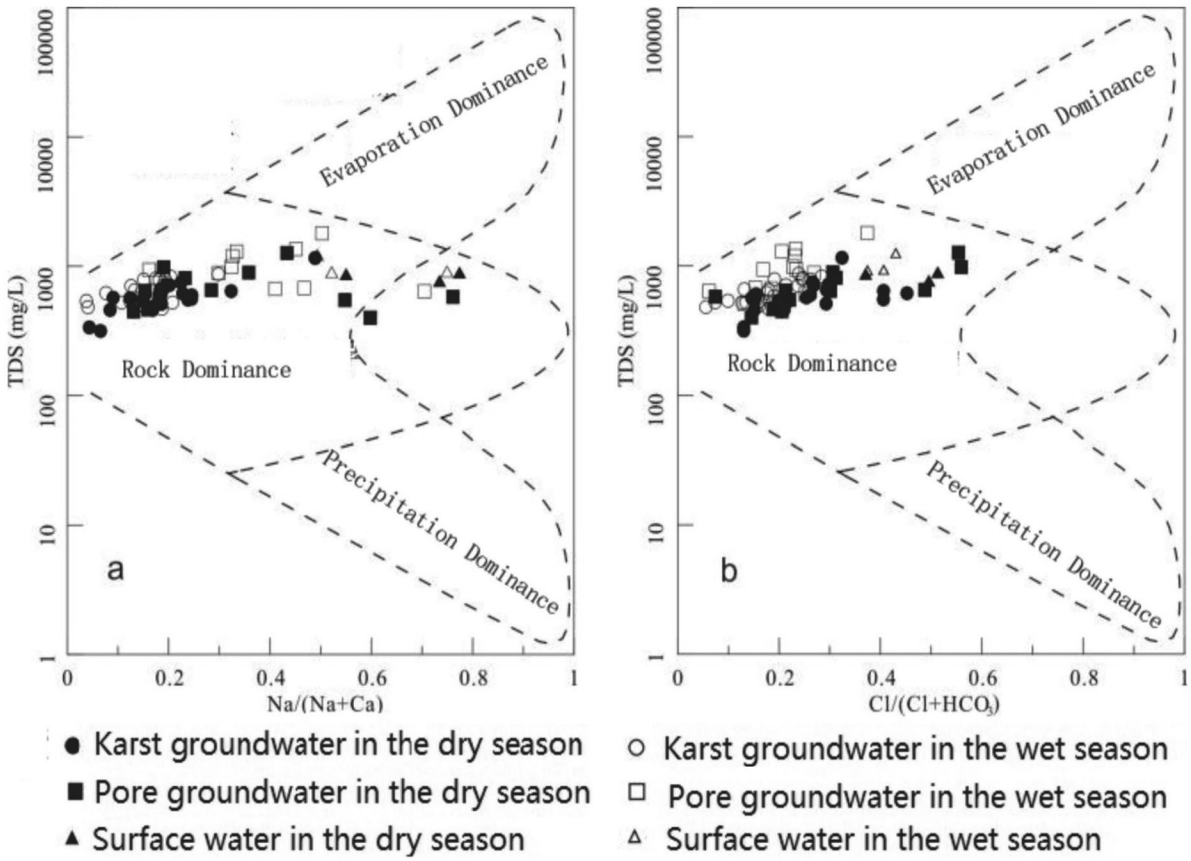

Fig. 5 Gibbs diagrams of groundwater samples in the study area

are $y=-0.523x+0.9399$ and $y=-1.3976x+1.3393$, in which R^2 is 0.2897 and 0.1877, respectively. The correlation equations of pore groundwater in the wet and dry seasons are $y=-1.0329x+1.1758$ and $y=-1.3511x+1.0595$, in which R^2 is 0.921 and 0.946 (Fig. 7a), respectively. Comparing and analyzing the correlation equations and correlation coefficients of karst groundwater and pore groundwater, pore groundwater appears to be more affected by cation exchange than karst groundwater.

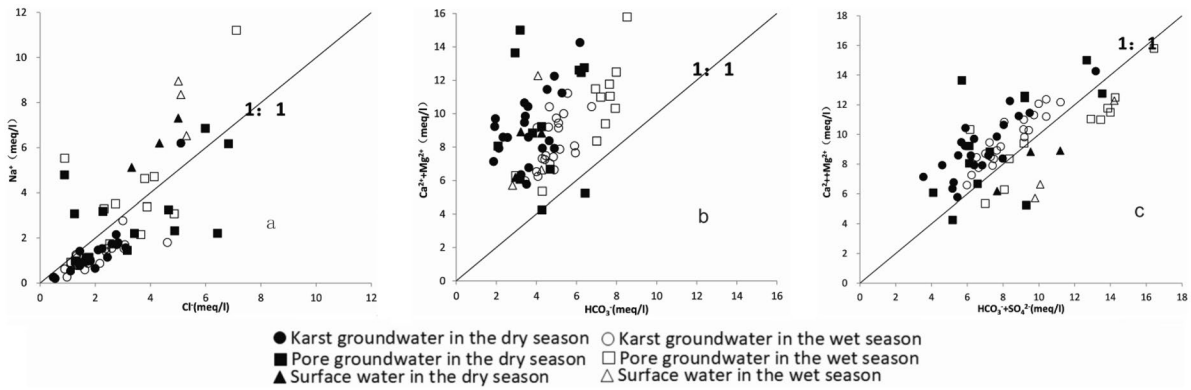

Fig. 6 Hydrochemical relationships between the rates of the selected ions of water samples

The expression of the chlor-alkali index is shown in formulas (1) and (2). When the chlor-alkali index is positive, the exchange of Na^+ and Ca^{2+} occurs according to formula (3); that is, when Ca^{2+} enters the groundwater, Na^+ is adsorbed by solid particles in the positive direction. When the chlor-alkali index is negative, Na^+ and Ca^{2+} exchange in the opposite direction (4). The greater the absolute value of the chlor-alkali index, the stronger the cation exchange effect. Figure 7b shows that the chlor-alkali index of most of the karst groundwater samples is positive (only two samples are negative in the dry season). This shows that the cation exchange of the karst groundwater is mainly in the positive direction, and the maximum value does not exceed 0.8, indicating that the exchange is not strong. The negative and positive values of the chlor-alkali index of pore groundwater are about half and half, which means both positive and negative directions of cation exchange are present. The reason for this may be related to pore groundwater's susceptibility to evaporation and human activities. The maximum value of CAI-1 in pore groundwater reached − 5.20, indicating that cation exchange in pore groundwater is stronger than karst groundwater.

$$\mathrm{CAI}-1=\frac{\mathrm{Cl}^- - (\mathrm{Na}^+ + \mathrm{K}^+)}{\mathrm{Cl}^-} \quad (1)$$

$$\mathrm{CAI}-1=\frac{\mathrm{Cl}^- - (\mathrm{Na}^+ + \mathrm{K}^+)}{\mathrm{Cl}^- + \mathrm{SO}_4^{2-} + \mathrm{CO}_3^{2-} + \mathrm{NO}_3^-} \quad (2)$$

$$2\mathrm{Na}^+ + \mathrm{CaX}_2 = \mathrm{Ca}^{2+} + 2\mathrm{NaX} \quad (3)$$

$$\mathrm{Ca}^{2+} + 2\mathrm{NaX} = 2\mathrm{Na}^+ + \mathrm{CaX}_2 \quad (4)$$

Human activities

Human activities that can affect the hydrochemical characteristics of groundwater in the study area include agricultural activities, karst groundwater extraction, and industrial production, each of which has direct or indirect effects on the formation of groundwater hydrochemistry. Fertilizers and pesticides used in agriculture enter the groundwater with precipitation infiltration, directly affecting the quality of groundwater. The average concentration of NO_3^- and Cl^- in pore groundwater in the study

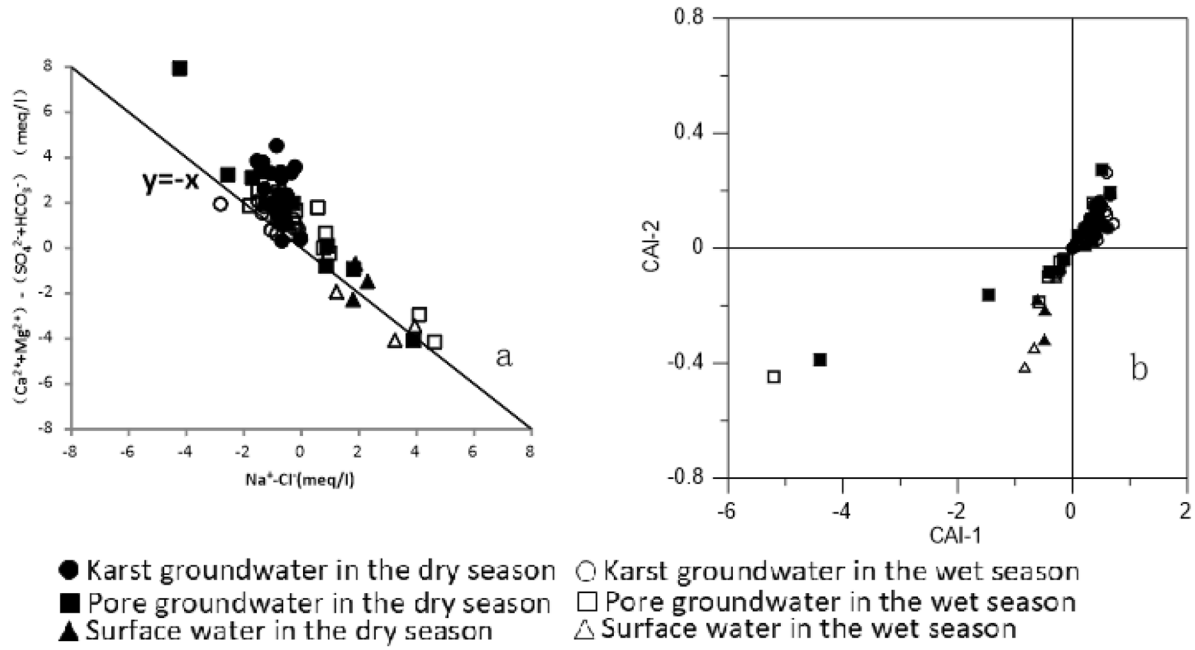

Fig. 7 Bivariate diagrams for studying cation exchange (**a** (Na^+–Cl^-) versus [(Ca^{2+} + Mg^{2+})–(HCO_3^- + $SO_4.^{2-}$)]; **b** CAI-1 versus CAI-2)

area is clearly greater than that in karst groundwater (Fig. 5). The NO_3^- concentration in karst groundwater gradually decreases from the mountainous areas to the piedmont plains (Fig. 4). Samples with higher NO_3^- concentrations are located in the groundwater replenishment area at the foot of the mountains which means that agricultural activities have an impact on karst groundwater chemistry. The urban and rural residents of Zoucheng City and the industrial enterprises of the Taiping industrial zone mainly use karst groundwater as a water supply source. The large-scale extraction of karst groundwater promotes water–rock interaction and cation exchange, which indirectly affects the hydrochemical characteristics of groundwater. Taiping Town in the northern part of the study area is a high-tech industrial zone in Zoucheng City with many industries, such as chemical, pharmaceutical, and paper production. These industries extract a large amount of karst groundwater and the discharge of sewage and wastewater from them will affect the quality of pore and karst groundwater.

Principal component analysis

Principal component analysis (PCA) is a multivariate statistical method that examines the correlation between multiple variables. It reveals the internal structure of multiple variables through a few principal components. It enables the user to derive a few key components from the original variables and then allows these components to preserve as much information as possible about the original variables independently of one another. This study contains 11 factors, the correlation between the factors is relatively strong, and the factors are continuous variables. Based on these traits, this study is best suited to principal component analysis. The selection of the factors is based on both the significance (eigenvalues > 1) of the factor and the cumulative percentage of data variance (cumulative percentage > 80%). Table 4 shows the PCA results of K^+, Na^+, Ca^{2+}, Mg^{2+}, Cl^-, SO_4^{2-}, HCO_3^-, F^-, NO_3^-, TDS, and TH during the dry and wet seasons of karst groundwater. For karst groundwater in the dry season, two principal components were extracted based on a characteristic value greater than 1, which explained 82.27% of the original variables. Among them, the principal components RC1 and RC2 explained 58.36% and 23.91% of the variance, respectively. The principal component RC1 has high correlation with Na^+, Mg^{2+}, Cl^-, SO_4^{2-}, HCO_3^-, F^-, TDS, and TH, and the correlation coefficients are 0.897, 0.971, 0.918, 0.894, 0.609, 0.802, 0.945, and 0.915, respectively. This represents the dissolution of salt rock, carbonate rock, and gypsum, indicating the occurrence of water–rock interaction (Wu et al., 2014, 2020). The main component RC2 is closely related to K^+, Ca^{2+}, and NO_3^-, and the correlation coefficients are 0.748, 0.824, and 0.939,

Table 4 The principal component analysis results of karst groundwater

Parameter	Dry season		Wet season		
	RC1	RC2	RC1	RC2	RC3
K^+	0.091	0.748	0.175	0.896	0.076
Na^+	0.897	0.137	0.851	−0.035	−0.058
Ca^{2+}	0.355	0.824	0.649	0.473	0.272
Mg^{2+}	0.971	−0.091	0.812	−0.378	−0.156
Cl^-	0.918	0.250	0.903	0.028	0.104
SO_4^{2-}	0.894	−0.229	0.801	−0.231	−0.456
HCO_3^-	0.609	0.257	0.490	0.047	0.779
F^-	0.802	−0.465	0.404	−0.251	−0.728
NO_3^-	−0.123	0.939	−0.198	0.939	0.150
TDS	0.945	0.315	0.977	0.193	0.018
TH	0.915	0.355	0.965	0.092	0.091
Eigenvalues	6.42	2.63	5.62	2.68	1.03
Variance explained (%)	58.36	23.91	51.13	24.33	9.39
Cum. var. explained (%)	58.36	82.27	51.13	75.46	84.85

respectively, representing human activities (such as pesticides, fertilizer use, and industrial wastewater discharge). For the karst groundwater in the wet season, three principal components were extracted based on a characteristic value greater than 1, which explained 84.85% of the variance. The principal components RC1 and RC2 explained 51.13% and 24.33% of the variance, respectively. The principal component RC1 has a high correlation with Na^+, Ca^{2+}, Mg^{2+}, Cl^-, SO_4^{2-}, TDS, and TH, and the correlation coefficients are 0.851, 0.649, 0.812, 0.903, 0.801, 0.977, and 0.965, respectively. The principal component RC2 has a high correlation with K^+ and NO_3^-, and the correlation coefficients are 0.896 and 0.939, respectively. It is clear that RC1 and RC2 in the wet season are caused by the same factors as RC1 and RC2 in the dry season, which are water–rock interaction and human activity influence, respectively. The principal component RC3, which explains 9.39% of the variance, has a high correlation with HCO_3^- and F^-. Some studies have speculated that CO_2 in precipitation promotes the dissolution of carbonate rocks and precipitation carries industrial wastewater into the aquifer (Ren et al., 2021). Therefore, RC3 indicates the influence of atmospheric precipitation.

Table 5 shows the PCA results of K^+, Na^+, Ca^{2+}, Mg^{2+}, Cl^-, SO_4^{2-}, HCO_3^-, F^-, NO_3^-, TDS, and TH during the dry and wet seasons of pore groundwater. For pore groundwater during the dry season, three principal components were extracted based on a characteristic value greater than 1, which explained 83.72% of the original variables. Among them, the principal components RC1, RC2, and RC3 explained 45.79%, 27.07%, and 10.86% of the variance, respectively. The main component RC1 has a high correlation with Na^+, Ca^{2+}, Mg^{2+}, Cl^-, SO_4^{2-}, TDS, and TH, and the correlation coefficients are 0.647, 0.636, 0.828, 0.919, 0.835, 0.989, and 0.916, respectively. This represents the dissolution of chlorine rock, magnesium rock, and gypsum; in other words, water–rock interactions (Ren et al., 2021; Wu et al., 2014, 2020). The main component RC2 is closely related to Na^+, Ca^{2+}, Mg^{2+}, HCO_3^-, F^-, and NO_3^-, and the correlation coefficients are 0.551, −0.647, 0.500, 0.814, 0.682, and −0.760, respectively. This indicates that the pore groundwater is affected by human activities such as industrial sewage, wastewater discharge, domestic sewage, agricultural activities, and mining. The principal component RC3 is closely related solely to K^+, with a correlation coefficient of 0.892, which may be due to the dissolution of silicate. For pore groundwater in the wet season, three principal components were extracted based on a characteristic value greater than 1, which explained 84.54% of the variance. The principal components RC1, RC2, and RC3 explained 51.71%, 22.30%, and 10.53% of the variance, respectively. The principal component RC1 also has a high correlation with Na^+, Ca^{2+}, Mg^{2+}, Cl^-, SO_4^{2-}, TDS, and TH, and the correlation coefficients

Table 5 The principal component analysis results of pore groundwater

Parameter	Dry season			Wet season		
	RC1	RC2	RC3	RC1	RC2	RC3
K^+	0.010	0.072	0.892	−0.059	0.724	0.231
Na^+	0.647	0.551	−0.362	0.768	−0.398	0.277
Ca^{2+}	0.636	−0.647	0.366	0.826	0.534	−0.087
Mg^{2+}	0.828	0.500	−0.100	0.601	−0.167	0.718
Cl^-	0.919	−0.253	0.139	0.927	0.009	0.156
SO_4^{2-}	0.835	−0.016	−0.153	0.955	−0.080	0.030
HCO_3^-	0.066	0.814	0.224	0.256	0.100	0.882
F^-	−0.074	0.682	−0.487	−0.205	−0.640	0.632
NO_3^-	0.223	−0.760	−0.018	0.064	0.721	−0.196
TDS	0.989	−0.128	0.035	0.964	0.113	0.201
TH	0.916	−0.249	0.234	0.890	0.337	0.240
Eigenvalues	5.04	2.98	1.19	5.69	2.45	1.16
Variance explained (%)	45.79	27.07	10.86	51.71	22.30	10.53
Cum. var. explained (%)	45.79	72.86	83.72	51.71	74.01	84.54

are 0.768, 0.826, 0.601, 0.927, 0.955, 0.964, and 0.890, respectively, indicating that the principal component RC1 is similar to that of the dry season. The main component RC2 has a high correlation with K^+, Ca^{2+}, F^-, and NO_3^-, and the correlation coefficients are 0.724, 0.534, 0.640, and 0.721, respectively. As in the dry season, it is affected by human activities such as industrial wastewater discharge, domestic sewage, agricultural activities, and mining activities. The main component RC3 has a high correlation with Mg^{2+}, HCO_3^-, and F^-, and the correlation coefficients are 0.718, 0.882, and 0.632, respectively, which may be affected by precipitation during the wet season.

Conclusions

1. On the whole, the concentrations of cations in both the karst groundwater and pore groundwater in the study area are in the order of $Ca^{2+} > Na^+ > Mg^{2+} > K^+$, while the concentrations of anions are in the order of $HCO_3^- > SO_4^{2-} > Cl^- > NO_3^- > F^-$. The chemical makeup of karst groundwater is quite different from that of pore groundwater. There are 7 hydrochemical types of karst groundwater in the dry season, mainly HCO_3-Ca and $HCO_3 \cdot SO_4$-Ca·Mg. There are 5 hydrochemical types in the wet season, of which the $HCO_3 \cdot SO_4$-Ca·Mg and $HCO_3 \cdot SO_4$-Ca types are predominant. HCO_3 and SO_4 type groundwater increases during the wet season compared with the dry season. The hydrochemical types of pore groundwater are complex and changeable. Compared with karst groundwater, the Na type water in pore groundwater is clearly more prevalent.
2. The indicators of Ca^{2+}, Na^+, Mg^{2+}, HCO_3^-, SO_4^{2-}, Cl^-, and TH in groundwater are highly correlated with TDS, while K^+, F^-, and NO_3^- have poor correlation with TDS, indicating that the former and the latter have different sources. The former is mainly affected by water–rock interactions, while the latter is mainly affected by human activities.
3. The formation of karst groundwater and pore groundwater is primarily affected by water–rock interactions and human activities, and secondly affected by cation exchange. The formation of 82.27% and 75.46% of karst groundwater in the dry and wet season respectively are affected by water–rock interactions and human activities. The formation of 72.86% and 74.01% of the pore groundwater are affected by water–rock interactions and human activities in dry and wet seasons, respectively. The main cation exchange direction in karst groundwater is positive, and the pore groundwater has both positive and negative directions. The cation exchange in the pore groundwater is stronger than that in the karst groundwater.

Funding This research is funded by the National Natural Science Foundation of China (Grant No. 42027806) and the Survey and Evaluation of Groundwater Sources Project in Shandong Province (Ludihuan (2016) No. 02).

Data availability The authors declare that the data supporting the findings of this study are available within the article.

Declarations

Competing interests The authors declare no competing interests.

References

Adimalla, N. (2019). Groundwater quality for drinking and irrigation purposes and potential health risks assessment: A case study from semi-arid region of South India. *Exposure and Health, 11,* 109–123. https://doi.org/10.1007/s12403-018-0288-8

Brindha, K., Rajesh, R., Murugan, R., & Elango, L. (2011). Fluoride contamination in groundwater in parts of Nalgonda District, Andhra Pradesh, India. *Environmental Monitoring and Assessment, 172,* 481–492. https://doi.org/10.1007/s10661-010-1348-0

Bouzourra, H., Bouhlila, R., Elango, L., Slama, F., & Ouslati, N. (2015). Characterization of mechanisms and processes of groundwater salinization in irrigated coastal area using statistics, GIS, and hydrogeochemical investigations. *Environmental Science and Pollution Research, 22,* 2643–2660. https://doi.org/10.1007/s11356-014-3428-0

Bu, H. (2000). Evaluation of groundwater environmental quality in Shuangcun karst water system of Zoucheng City. *Geology of Shandong, 1,* 44–50 (in Chinese).

Civita, M. V. (2008). An improved method for delineating source protection zones for karst springs based on analysis of recession curve data. *Hydrogeology Journal, 16,* 855–869. https://doi.org/10.1007/s10040-008-0283-4

Deiana, M., Cervi, F., Pennisi, M., et al. (2018). Chemical and isotopic investigations ($\delta^{18}O$, δ^2H,^3H,$^{87}Sr/^{86}Sr$) to define groundwater processes occurring in a deep-seated landslide in flysch. *Hydrogeology Journal, 26*, 2669–2691. https://doi.org/10.1007/s10040-018-1807-1

Escolero, O. A., Marin, L. E., Steinich, B., Pacheco, A. J., Cabrera, S. A., & Alcocer, J. (2002). Development of a

protection strategy of karst limestone aquifers: The Merida Yucatan, Mexico case study. *Water Resources Management, 16,* 351–367. https://doi.org/10.1023/A:1021967909293

Gibbs, R. J. (1970). Mechanisms controlling world water chemistry. *Science, 170*(3962), 1088–1090. https://doi.org/10.1126/science.170.3962.1088

Hassen, I., Hamzaoui-Azaza, F., & Bouhlila, R. (2016). Application of multivariate statistical analysis and hydrochemical and isotopic investigations for evaluation of groundwater quality and its suitability for drinking and agriculture purposes: Case of Oum Ali-Thelepte aquifer, central Tunisia. *Environmental Monitoring and Assessment, 188,* 135. https://doi.org/10.1007/s10661-016-5124-7

He, S., & Li, P. (2020). A MATLAB based graphical user interface (GUI) for quickly producing widely used hydrogeochemical diagrams. *Geochemistry, 80*(4), Supplement, 125550. https://doi.org/10.1016/j.chemer.2019.125550

He, X., Wu, J., & Guo, W. (2019). Karst spring protection for the sustainable and healthy living: The examples of Niangziguan spring and Shuishentang spring in Shanxi, China. *Exposure and Health, 11,* 153–165. https://doi.org/10.1007/s12403-018-00295-4

Li, C.-C., Gao, X.-B., & Wang, Y.-X. (2015). Hydrogeochemistry of high-fluoride groundwater at Yuncheng Basin, northern China. *Science of the Total Environment, 508,* 155–165. https://doi.org/10.1016/j.scitotenv.2014.11.045

Li, P.-Y., He, X.-D., & Guo, W.-Y. (2019). Spatial groundwater quality and potential health risks due to nitrate ingestion through drinking water: A case study in Yan'an City on the Loess Plateau of northwest China. *Human and Ecological Risk Assessment, 25*(1–2), 11–31. https://doi.org/10.1080/10807039.2018.1553612

Li, P.-Y., Tian, R., & Liu, R. (2019). Solute geochemistry and multivariate analysis of water quality in the Guohua phosphorite mine, Guizhou Province, China. *Exposure and Health, 11*(2), 81–94. https://doi.org/10.1007/s12403-018-0277-y

Li, P.-Y., Wu, J.-H., Qian, H., Zhang, Y.-T., Yang, N., Jing, L.-J., & Yu, P.-Y. (2016). Hydrogeochemical characterization of groundwater in and around a wastewater irrigated forest in the southeastern edge of the Tengger Desert, northwest China. *Exposure and Health, 8,* 331–348. https://doi.org/10.1007/s12403-016-0193-y

Li, P.-Y., Zhang, Y.-T., Yang, N., Jing, L.-J., & Yu, P.-Y. (2016). Major ion chemistry and quality assessment of groundwater in and around a mountainous tourist town of China. *Exposure and Health, 8,* 239–252. https://doi.org/10.1007/s12403-016-0198-6

Liang, Y.-P., & Zhao, C.-H. (2018). Karst water function in northern China. *China Mining Magazine, 27,* 297–299. https://doi.org/10.12075/j.issn.1004-4051.2018.S2.078 (in Chinese).

Liu, W.-J., Yuan, X.-M., Zhang, Y., et al. (2018). Hydrochemical characteristics and evolution of karst groundwater in Guiyang City. *Geological Science and Technology Information, 37*(6), 245–251. https://doi.org/10.19509/j.cnki.dzkq.2018.0631 (in Chinese).

Liu, F., Song, X.-F., & Yang, L.-H. (2015). The role of anthropogenic and natural factors in shaping the geochemical evolution of groundwater in the Subei Lake basin, Ordos energy base, Northwestern China. *Science of the Total Environment, 538,* 327–340. https://doi.org/10.1016/j.scitotenv.2015.08.057

Luo, F., Su, C.-T., Pan, X.-D., et al. (2018). Hydrochemical characteristics and geochemical sensitivity of groundwater in typical karst hilly regions: A case study of Eastern Wugang. *Carsologica Sinica, 37*(2), 211–217. https://doi.org/10.11932/karst20180207 (in Chinese).

Lü, W., Yao, X., Su, C., et al. (2020). Characteristics and influencing factors of hydrochemistry and dissolved organic matter in typical karst water system. *Environmental Science and Pollution Research, 27,* 11174–11183. https://doi.org/10.1007/s11356-019-07227-y

Maramathas, A. (2006). A new approach for the development and management of brackish karst springs. *Hydrogeology Journal, 14,* 1360–1366. https://doi.org/10.1007/s10040-006-0048-x

Marghade, D., Malpe, D. B., & Zade, A. B. (2012). Major ion chemistry of shallow groundwater of a fast growing city of Central India. *Environmental Monitoring and Assessment, 184,* 2405–2418. https://doi.org/10.1007/s10661-011-2126-3

Ministry of Ecological and Environment. (2009). *Water quality sampling — technical regulation of the preservation and handling of samples (HJ 493–2009)*. Beijing: China Environment Publishing Group.

Plagnes, V., & Bakalowicz, M. (2002). The protection of a karst water resource from the example of the Larzac karst plateau (south of France): A matter of regulations or a matter of process knowledge? *Engineering Geology, 65,* 107–116. https://doi.org/10.1016/S0013-7952(01)00117-X

Rajesh, R., Brindha, K., & Elango, L. (2015). Groundwater quality and its hydrochemical characteristics in a shallow weathered rock aquifer of southern India. *Water Quality Exposure and Health, 7,* 515–524. https://doi.org/10.1007/s12403-015-0166-6

Reddy, A. G. S., & Kumar, K. N. (2010). Identification of the hydrogeochemical processes in groundwater using major ion chemistry: A case study of Penna-Chitravathi River basins in southern India. *Environmental Monitoring and Assessment, 170,* 365–382. https://doi.org/10.1007/s12665-020-08913-8

Ren, X., Li, P., He, X., Su, F., & Elumalai, V. (2021). Hydrogeochemical processes affecting groundwater chemistry in the central part of the Guanzhong Basin, China. *Archives of Environmental Contamination and Toxicology, 80*(1), 74–91. https://doi.org/10.1007/s00244-020-00772-5

Salem, Z. E., Atwia, M. G., & El-Horiny, M. M. (2015). Hydrogeochemical analysis and evaluation of groundwater in the reclaimed small basin of Abu Mina, Egypt. *Hydrogeology Journal, 23*(8), 1–17. https://doi.org/10.1007/s10040-015-1303-9

Sheikhy Narany, T., Bittner, D., Disse, M., et al. (2019). Spatial and temporal variability in hydrochemistry of a small-scale dolomite karst environment. *Environment and Earth Science, 78*, 273. https://doi.org/10.1007/s12665-019-8276-2

Sheng, Y., He, J.-T., Wang, J.-J., et al. (2013). Hydrochemical characteristics of groundwater based on multivariate statistical analyses: Taking the Liguanpu Ripanian wellhead area in Shenyang city for example. *Geoscience, 27*(2), 440–447 (in Chinese).

Smith, D. N., Ortega-Camacho, D., Acosta-González, G., Leal-Bautista, R. M., Fox, W. E., & Cejudo, E. (2020). A multi-approach assessment of land use effects on groundwater quality in a karstic aquifer. *Heliyon, 6,* e03970. https://doi.org/10.1016/j.heliyon.2020.e03970

Ventura-Houle, R., Guevara-Mansilla, O., Requena-Lara, G., et al. (2021). Hydrochemistry, δD and δ18O to explain the distribution of water quality in a karst setting in the semi-arid region of Northeast Mexico. *Environment and Earth Science, 80,* 6. https://doi.org/10.1007/s12665-020-09310-x

Wang, H., Jiang, X.-W., Wan, L., Han, G.-L., & Guo, H.-M. (2015). Hydrogeochemical characterization of groundwater flow systems in the discharge area of a river basin. *Journal of Hydrology, 527,* 433–441. https://doi.org/10.1016/j.jhydrol.2015.04.063

Wang, X. X., Wang, W. K., Wang, Z. F., et al. (2014). Hydrochemical characteristics and formation mechanism of river water and groundwater along the downstream Luanhe River [J]. *Hydrogeology & Engineering Geology, 041*(001):25–33, 73. https://doi.org/10.16030/j.cnki.issn.1000-3665.2014.01.005. (in Chinese).

Wu, J., Li, P., Qian, H., Duan, Z., & Zhang, X. (2014). Using correlation and multivariate statistical analysis to identify hydrogeochemical processes affecting the major ion chemistry of waters: Case study in Laoheba phosphorite mine in Sichuan, China. *Arabian Journal of Geosciences, 7*(10), 3973–3982. https://doi.org/10.1007/s12517-013-1057-4

Wu, J., Li, P., Wang, D., Ren, X., & Wei, M. (2020). Statistical and multivariate statistical techniques to trace the sources and affecting factors of groundwater pollution in a rapidly growing city on the Chinese Loess Plateau. *Human and Ecological Risk Assessment, 26*(6), 1603–1621. https://doi.org/10.1080/10807039.2019.1594156

Yang, Q.-C., Li, Z.-J., Ma, H.-Y., Wang, L.-C., & Martín, J. D. (2016). Identification of the hydrogeochemical processes and assessment of groundwater quality using classic integrated geochemical methods in the southeastern part of Ordos basin, China. *Environmental Pollution, 218,* 879–888. https://doi.org/10.1016/j.envpol.2016.08.017

Yuan, J.-F., Deng, G.-S., Xu, F. et al. (2016). The multivariate statistical analysis of chemical characteristics and influencing factors of karst groundwater in the northern part of Bijie City, Guizhou Province. *Geology in China, 43*(4),1446–1456. https://doi.org/10.12029/gc20160428 (in Chinese)

Zang, H., Zheng, X., Jia, Z., Chen, J., & Qin, Z. (2015). The impact of hydrogeochemical processes on karst groundwater quality in arid and semiarid area: A case study in the Liulin spring area, north China. *Arabian Journal of Geosciences, 8,* 6507–6519. https://doi.org/10.1007/s12517-014-1679-1